Pulverized river shellfish shells as a cheap adsorbent for removing of malathion from water: Examination of the isotherms, kinetics, thermodynamics and optimization of the experimental conditions by the response surface method

Veli#kovi#, Zlate S.; Vuji#i#, Bogdan D.; Stojanovi#, Vladica N.; Stojisavljevi#, Predrag N.; Baji#, Zoran J.; #oki#, Veljko R.; Ivankovi#, Negovan D.; Otrisal, Pavel P.

Pulverized river shellfish shells as a cheap adsorbent for removing of malathion from water: Examination of the isotherms, kinetics, thermodynamics and optimization of the experimental conditions by the response surface method

Измельченные раковины пресноводных моллюсков в качестве дешевого адсорбента для удаления малатиона из водной среды: исследования изотермы, кинетики, термодинамики и оптимизация экспериментальных условий методом поверхности реагирования

Спрашене љуштуре речних шкољки као јефтини адсорбент заузклањање малатиона из воде: испитивање изотерми, кинетике, термодинамике и оптимизација експерименталних условаметодом одзивних површина

Zlate S. Veličković
University of Defence in Belgrade, Serbia
zlatevel@yahoo.com
https://orcid.org/0000-0001-5335-074X

Bogdan D. Vujičić
University of Defence in Belgrade, Serbia
bogdanvujicic47@gmail.com
https://orcid.org/0000-0003-3026-4544

Vladica N. Stojanović
University of Defence in Belgrade, Serbia
vllajkoo.vs@gmail.com
https://orcid.org/0000-0002-9844-2477

Predrag N. Stojisavljević
Serbian Armed Forces, Serbia
pedjastojis@yahoo.com
https://orcid.org/0000-0002-1170-7912

Zoran J. Bajić
University of Defence in Belgrade, Serbia
angrist2@gmail.com
https://orcid.org/0000-0002-8492-3333

Veljko R. Đokić
University of Belgrade, Serbia
vdjokic@tmf.bg.ac.rs
https://orcid.org/0000-0003-2541-0420

Negovan D. Ivanković
University of Defence in Belgrade, Serbia
negovan.ivankovic@gmail.com
https://orcid.org/0000-0003-0202-8210

AUTHOR NOTES

zlatevel@yahoo.com

Pavel P. Otrisal
Palacky University, Czech Republic
pavel.otrisal@upol.cz
https://orcid.org/0000-0002-9345-3978

ABSTRACT:

Introduction/purpose: In this study, we investigated the possibility of removing the organophosphorus pesticide malathion from water using a new adsorbent based on the biowaste of river shell shards from the Anodonta Sinadonta woodiane family, a material that accumulates in large quantities as waste on the banks of large rivers. Two adsorbents were tested - mechanically comminuted river shells (MRM) and mechanosynthetic hydroxyapatite from comminuted river shells (RMHAp).

Methods: The obtained adsorbents were characterized and tested for the removal of the organophosphorus pesticide malathion from water. In order to predict the optimal adsorption conditions using the Response Surface Method (RSM), the authors investigated the influence of variable factors (adsorption conditions), pH values, adsorbent doses, contact times, and temperatures on the adsorbent capacity.

Results: The best adsorption of malathion was achieved at mean pH values between 6.0 and 7.0. The adsorption data for malathion at 25, 35, and 45 °C were compared using the Langmuir, Freundlich, Dubinin-Radushkevich (DR), and Temkin isothermal models, as well as pseudo-first order, pseudo-second order and Elovic kinetic models for modeling adsorption kinetics. The maximum Langmuir adsorption capacity for MRM and RMHAp at 25 °C was 46,462 $mg\,g^{-1}$ and 78,311 $mg\,g^{-1}$, respectively.

Conclusion: The results have showed that malathion adsorption on both adsorbents follows the pseudo-second kinetic model and the Freundlich isothermal model. The thermodynamic parameters indicate the endothermic, feasible, and spontaneous nature of the adsorption process.

KEYWORDS: removal, adsorbent, kinetics, isotherms, optimization, pesticide, water, river shells.

Р е з ю м е :

Введение/цель: В данной статье представлены результаты исследования возможности удаления фосфорорганического пестицида малатиона из водной среды с помощью нового адсорбента на основе биоотходов − раковин пресноводных моллюсков семейства Anodonta Sinadonta woodiane, материала, который в больших количествах накапливается в виде отходов на побережьях крупных рек.

Методы: Были испытаны два адсорбента − механически измельченные речные раковины (MRM) и гидроксиапатит из измельченных речных раковин, полученный механосинтезом (RMHAp). Полученные адсорбенты были исследованы (элементный анализ, сканирующая электронная микроскопия − SEM, энергодисперсионная рентгеновская спектроскопия − EDS, рентгеноструктурный анализ − HRD, инфракрасная спектроскопия с преобразованием Фурье (ИКФС, FTIR) и испытаны методом прерывания на удаление органофосфорного пестицида малатиона из водной среды. Оптимизация условий адсорбции проводилась методом поверхностей отклика − RSM, при этом исследовалось влияние переменных факторов (условий адсорбции), значений pH, доз адсорбента, времени контакта и температуры на адсорбционную способность адсорбента.

Результаты: Наилучшая адсорбция малатиона была достигнута при средних значениях pH от 6,0 до 7,0. Максимальная адсорбционная способность Ленгмюра по MRM и RMHAp при 25 °C составляла 46 462 мг г$^{-1}$ и 78 311 мг г$^{-1}$. Результаты показали, что адсорбция малатиона на обоих адсорбентах соответствует кинетической модели псевдо-второго порядка и модели изотермы Фрейндлиха. Термодинамические параметры указывают на эндотермический, самопроизвольный характер, приемлемый в процессе адсорбции.

Выводы: В ходе исследования был получен дешевый биосовместимый адсорбент с отличными адсорбционными свойствами в отношении малатиона. Таким образом из отходов моллюсков извлекается двойная выгода: используются отходы, которыми завалены побережья различных водотоков, и удаляются загрязняющие воду вещества, оказывающие негативное воздействие на окружающую среду в целом.

К л ю ч е в ы е   с л о в а : удаление, адсорбент, кинетика, изотермы, оптимизация, пестициды, вода, пресноводные моллюски.

ABSTRACT:

Увод/циљ: У овом истраживању испитиване су могућности уклањања органофосфорног пестицида малатиона из воде помоћу нових адсорбената на бази биоотпада речних шкољки из породице Anodonta Sinadonta woodiane, материјала који се у великим количинама накупља као отпад на обалама великих река.

Методе: Синтетисана су два адсорбента: механички уситњена речна шкољка (MRM) и хидроксиапатит добијен механосинтезом из уситњених речних шкољки (RMHAp). Добијени адсорбенти су окарактерисани (елементарна анализа, скенирајућа електронска микроскопија – СЕМ, електродисперзивна спектроскопија – ЕДС, рендгенска дифракциона анализа – ХРД, Фуријева трансформација ИР зрака – ФТИР) и испитани у шаржном систему за уклањање органофосфорног пестицида малатиона из воде. Оптимизација услова адсорпције извршена је методом одзивних површина – РСМ, где је испитан утицај променљивих фактора (услова адсорпције), пХ вредности, дозе адсорбента, времена контакта и температуре на капацитет адсорбента.

Резултати: Најбоља адсорпција малатиона постигнута је при средњим пХ вредностима између 6,0 и 7,0. Максимални Лангмуиров капацитет адсорпције за MRM и RMHAp на 25°Ц износио је 46,462 мг г$^{-1}$ и 78,311 мг г$^{-1}$, редом. Резултати су показали да адсорпција малатиона на оба адсорбента следи псеудодруги кинетички модел и Фројндлихов изотермни модел. Термодинамички параметри указују на ендотермну, спонтану и изводљиву природу процеса адсорпције.

Закључак: У току истраживања добијен је јефтин биокомпатибилни адсорбент са одличним адсорпционим карактеристикама према малатиону. Коришћење отпада од шкољки врло је корисно: јер отпад који оптерећује обале различитих водотокова уклања загађиваче који оптерећују воду и изазивају негативне ефекте на животну средину уопште.

KEYWORDS: уклањање, адсорбент, кинетика, изотерме, оптимизација, пестициди, вода, речне шкољке.

Introduction

The development of technology undoubtedly contributes to the development of society; however, it also causes environmental pollution. A distinct surge in the world's population and an increase in food needs condition the development of intensive agricultural production based on the use of inputs to overcome factors that limit production such as insects, fungi, weeds, and land scarcity (Kamga, 2019). The usage of pesticides is intended to combat animals and plants that are harmful to crops, thus enabling increased yields and ensuring the sustainability of the human population. Non-selective use of pesticides in agricultural activities leads to the pollution of surface and underground water accumulations. Due to its potential danger to health by entering the food chain for humans and animals, pesticide pollution has reached alarming proportions. (Chatterjee et al, 2010)

Pesticides are ecologically very important because of their high toxicity to living organisms, including humans; the toxicological profile of this pollutant poses a potential risk to the environment and public health (Kamga, 2019). According to numerous studies, many insecticides such as DDT, deildrin, heptachlor, and aldrin bioaccumulate in blood, milk, and tissues and are also found in food products (Singh et al, 2010).

It has been confirmed that patients with acute organophosphate poisoning suffer from problems such as vomiting, nausea, miosis, excessive salivation, blurred vision, headache, dizziness, and disturbances of consciousness (Singh et al, 2010). In the case of malathion, which is one of widely used organophosphorus pesticides, almost all the observed effects occur due to its active metabolite malacon (Singh et al, 2010) on the nervous system or gives secondary effects to its primary action.

Malathion is slowly absorbed through the skin, but is more rapidly and efficiently absorbed via ingestion. Once they are absorbed, phosphorothioates such as malathion are metabolically activated to the "oxon" forms which have greater toxicity than the parent insecticide. The metabolism of malathion leads to the formation of malathion monocarboxylic acid, malathion dicarboxylic acid, dialkyl phosphate metabolites, and other metabolites (Bouchard et al, 2003).

In recent years, research on the removal of pollutants from water has been intensified, based on the phenomenon of adsorption, among which the removal of pesticides from water occupies a special place. We have a large number of potentially highly effective adsorbents for removing pesticides from water such as activated carbon (Kamga, 2019; Ohno et al, 2008; Hameed et al, 2009), but the high price of activated carbon limits its mass use in many poor countries. Therefore, the attention of researchers is increasingly focused

on finding a cheap, environmentally friendly, and highly efficient adsorbent to solve this problem. Various adsorbents such as agricultural by-products, waste materials, cheap minerals and biomass have been used to remove various pollutants from wastewater (Chatterjee et al, 2010; Pantić et al, 2019; Bajić et al, 2013; Stevanović et al, 2020; Karanac et al, 2018; Perendija et al, 2021).

Malathion, an organophosphorus highly selective insecticide, is widely used in agriculture worldwide (Chatterjee et al, 2010), primarily in the control of insects, including mosquitoes, aphids, grass insects, and many other parasites of vegetable crops and fruits. Until today, the removal of malathion from wastewater has not been studied in detail and only a few studies are available in this regard (Chatterjee et al, 2010).

The shards of river shells are waste that burdens a large number of beaches and the banks of rivers, seas, and lakes. They also appear as waste after use in human nutrition. The aim of this paper is to apply shellfish as a cheap, widely available, environmentally friendly material for removing organophosphorus pesticides from water. In this way, we get a double benefit: we use waste that burdens the shores of different watercourses to remove pollutants that load the water and cause negative effects on life and health of humans and animals as well as on the environment in general.

Materials and methods

Materials

A large number of different chemicals were used during the research. Bearing in mind that the properties of the adsorbent, as well as the research results largely depend on the purity of the reagent, high purity chemicals were used:

- 5% hydrogen peroxide solution - H_2O_2 (Sigma-Aldrich, PA),
- concentrated nitric acid HNO_3. (Fluka, ultrapure) - used for digestion of shells in order to determine the elemental composition and adjust the pH level,
- concentrated phosphoric acid H_3PO_4 (Sigma-Aldrich, PA),
- sodium hydroxide - NaOH (Sigma Aldrich, PA) - used to adjust the pH of the solution in the adsorption process and titration during the synthesis of adsorbents,
- 96% ethyl alcohol (Sigma Aldrich, PA) - used in the washing of adsorbents,
- deionized water (resistance of 18 MΩ cm) - used for sample preparation and dilution of the solution,
- malathion, 60% technical solution (Galenika-Fitofarmacija) – used for performing an adsorption experiment (as 20 mg dm^{-3} concentration solution),
- biowaste of shellfish from the genus *Anodonta Sinadonta woodiane*, collected from the banks of the Tisza River.

Synthesis of adsorbents

During the research, two types of adsorbents based on river shell shards were synthesized and tested in the process of adsorption:

1. shells, washed, mechanically ground, sieved, washed, and dried in a vacuum oven - clean shells (MRM), and

2. fish carp scales chemically modified by converting calcium carbonate to hydroxyapatite by mechanosynthesis (RMHAp).

The shards of the *Anodonta Sinadonta woodiane* river shell were thoroughly washed and rinsed in distilled water, air-dried for 24 h, ground in a steel mill for crushing sediments and sifted into a 0.5 -1 mm granulation

PDF generated from XML JATS4R by Redalyc
Project academic non-profit, developed under the open access initiative
874

powder. The shell powder was washed in vacuo with deionized water, ethyl alcohol and dried in vacuo for 24 h at 110 ^{0}C to give the first MRM adsorbent (mechanically prepared river shells).

In the stainless steel vessel of a planetary ball mill (Retsch PM100 CM), 10 g of MRM was mixed with 11.23 ml (18.92 g) of concentrated H_3PO_4 - $CaCO_3$ ratio: H_3PO_4 → Ca / P = 1.67; zirconium beads were added in ratio 20:1 of the bead mass to a sample and the mixture was treated in a ball mill for 10 h at 500 grp for further mechanosynthesis. After the treatment in a ball mill, the obtained mixture was washed copiously in vacuo with deionized water to remove unreacted parts of the acid and dried in vacuo for 24 h at 110 °C to obtain a second RMHAp adsorbent (hydroxyapatite).

Material characterization methods

The synthesized adsorbents were characterized by FTIR, XRD, SEM and EDS techniques. The elemental composition was determined by a chemical elemental analyzer, the content of individual elements was determined by dissolving in acids and measuring the content on a plasma mass spectrometer with a plasma-coupled plasma ICP-MS system Agilent 7500C (Agilent Technologies, Inc.) and an atomic adsorption spectrometer. The concentration of malathion before and after adsorption was determined using a gas chromatograph (GC) equipped with a flame ionization detector (FID) - Varian 3400 with FID operating system. The specific surface area of the adsorbent, the specific pore volume, and the pore diameter were determined by the BET method of adsorption / desorption in a stream of nitrogen at 72.4 K, using a gas sorption analyzer Micromeritics ASAP 2020MP v 1.05 H. The infrared Fourier transform spectrum (FTIR) was recorded in the transformation mode between 400 and 4000 cm-1 at a resolution of 4 cm-1 using an infrared (IR) spectrometer with Fourier transformation (FT) - Nicolet iS 50 manufactured by Thermo Scientific. The adsorbents morphology was observed using Tescan Mira 3 FEG scanning electron field microscopy (FESEM). The morphological structure was determined by x-ray diffraction, XRD, using an ENRAF NONIUS FR590 XRD (Bruker AKSS, MA, USA) diffractometer with Cu Ka 1,2 radiation and a step / scan time regime of 0.05 / 1 s. The pH value of the zero charge point (pHPZC) of adsorbents was determined by the "drift" method (Gao et al, 2009).

Malathion adsorption research

Adsorption experiments were performed in a batch system where the initial concentration of malathion solution was fixed Co = 20.32 mg L^{-1}, and the adsorbent dose was varied from 100 to 1000 mg L^{-1}. In order to examine the pH value influence on the adsorption process, the pH value was varied from 4.0 to 10.0. Thermodynamic and kinetic adsorption experiments were performed at temperatures of 25, 35 and 45 ^{0}C, and the adsorption process was monitored in a time interval of 10 to 180 minutes. The amount of adsorbed molecules was calculated as the difference between the initial and equilibrium concentration.

The adsorbent capacity was calculated in accordance with Eq. (1):

$$q = \frac{C_i - C_f}{m} V$$

(1)

where q is the adsorption capacity in mg g^{-1}, C_i and C_f are the initial and final malathion concentrations in mg L^{-1} (μg L^{-1}), respectively, V is the volume of the solution in L, and . is the adsorbent mass, expressed in g.

Kinetic studies

The study of kinetics provides an insight into a possible mechanism of adsorption along with the reaction pathways. The adsorption data were analyzed by linear, non-linear least-squares and graphic methods in the form of pseudo-first, pseudo-second-order (Lagergreen) and second order models (Table 1).

Diffusion models such as Weber-Morris, Dunwald-Wagner model, and Homogenous Solid Diffusion Model (HSDM) were used for modeling diffusional processes/limiting step of the overall process (Table 2) (Budimirović et al, 2017; Taleb et al, 2015; Taleb et al, 2019).

TABLE 1
Kinetic model equations

Kinetic model	Nonlinear form	Model parameters	Equation
Pseudo-first-order equation	$q = q_e(1 - e^{-k_1 t})$	k_1- pseudo first-order rate constant, (min^{-1}) q_e- adsorption capacity at time t, (mg g^{-1}) q- adsorption capacity, (mg g^{-1}) t - time, (min)	(2)
Pseudo-second order equation (*Lagergreen*)	$q = \dfrac{t}{\dfrac{1}{k_2 q_e^2} + \dfrac{t}{q_e}}$	k_2 - pseudo-second order rate constant, (g mg^{-1} min^{-1})	(3)
Second order	$q = \dfrac{t}{\dfrac{1}{k_2 q_e^2} + \dfrac{t}{q_e}}$	k_2 - second order rate constant, (L mg^{-1} min^{-1})	(4)

TABLE 2
Equations of the diffusion kinetic models

Kinetic model	Nonlinear form	Equation
Weber-Morris	$q = k\sqrt{t} + C$	(5)
Dunwald-Wagner model	$\dfrac{q}{q_e} = 1 - \dfrac{6}{\pi^2} \sum\limits_{n=1}^{\infty} \dfrac{1}{n^2} exp[-n^2 K t]$ $log\left(1 - \left(\dfrac{q}{q_e}\right)^2\right) = -\dfrac{K}{2.303}t$	(6)
Homogenous Solid Diffusion Model (HSDM)	$\dfrac{\partial q}{\partial t} = \dfrac{D_s}{r^2}\dfrac{\partial}{\partial r}\left(r^2 \dfrac{\partial q}{\partial r}\right)$ $\dfrac{q}{q_s} = 1 + \dfrac{2R}{\pi r} \sum\limits_{n=1}^{\infty} \dfrac{(-1)^n}{n} sin\dfrac{n\pi r}{R} exp\left[\dfrac{-D_s t \pi^2 n^2}{R^2}\right]$	(7)

The activation energy for arsenate adsorption was calculated using Arrhenius (Eq. 8):

$$k^` = k_0 \exp \left[\frac{-E_a}{RT}\right]$$

(8)

where k' (g mg^{-1} min^{-1}) is the pseudo-second order rate adsorption constant, k_0 (g mmol^{-1} min^{-1}) is the temperature independent factor, E_a (kJ mol^{-1}) is the activation energy, R (8.314 J mol^{-1} K^{-1}) is the gas constant, and T(K) is the adsorption absolute temperature. A plot of ln K versus 1/T gave a straight line with a slope $-E_a$/R from which the activation energy was calculated.

Isotherm models

The equilibrium adsorption data were fitted by the isotherm models Langmuir, Freundlich, Temkin, and Dubinin-Radushkevich isothermal models (Karanac et al, 2018).

The Langmuir equation is based on the assumption that the point of maximum adsorption corresponds to a saturated mono-layer of adsorbate molecules on the adsorbent surface - where the energy of adsorption remains constant and no transfer of the adsorbate in the surface plane occurs.

The Freundlich sorption isotherm, widely and reliably utilized as a mathematical determining expression, allows for a calculation encompassing surface heterogeneity and exponential distribution of active sites as well as their respective energies (Karanac et al, 2018).

Temkin conceived this equation for subcritical vapors in micropore solids where the adsorption process follows a pore filling mechanism onto an energetically non-uniform surface.

The Temkin isotherm is based on the assumption that the decline of the heat of sorption as a function of temperature is linear rather than logarithmic. The Dubinin-Radushkevich model states that the adsorption capacity depends on the adsorbed amount on the surface of the material, differently from the Langmuir model." (Karanac et al, 2018).

The equations of adsorption isotherms models are presented in Table 3.

TABLE 3
Adsorption isotherms equations

Isotherms	Nonlinear form	Model parameters	Equation
Langmuir	$q_e = \dfrac{q_m K_L C_e}{1 + K_L C_e}$	q_e- adsorption capacity at th eequilibrium, (mg g^{-1}) q_m- maximum adsorption capacity, (mg g^{-1}) K_L- Langmuir equilibrium constant, (L mg^{-1}) C_e- metal ion concentration at the equilibrium (mg L^{-1})	(9)
Freundlich	$q = K_F C^{1/n}$	K_F- Freundlich equilibrium constant, (mg g^{-1})(L mg^{-1})$^{1/n}$ n- Freundlich equilibrium constant (intensity of the adsorption or surface heterogeneity)	(10)
Temkin	$q_e = \dfrac{RT}{b} \ln(A C_e)$	A -Temkin isotherm equilibrium binding constant (L g^{-1}) b - Temkin isotherm constant R-universal gas constant (8.314J mol^{-1}K^{-1}) T-Temperature at 298K.	(11)
Dubinin-Radushkevich	$q_e = q_m \exp\left(-B(RT)^2\left[\ln\left(1 + \dfrac{1}{C_e}\right)\right]^2\right)$		(12)

Thermodynamic studies

The feasibility of the experimental data obtained from the adsorption studies were analyzed through the thermodynamic investigation. The parameters of free energy change ($\Delta G°$, kJ/mol), enthalpy change ($\Delta H°$, kJ mol^{-1}), and entropy change ($\Delta S°$, J mol^{-1}K^{-1}) were calculated using the Van't Hoff equations (13) and (14) (Karanac et al, 2018):

$$\Delta G^0 = -RT \ln(b) \tag{13}$$

$$\ln(b) = \frac{\Delta S^0}{R} - \frac{\Delta H^0}{(RT)} \tag{14}$$

The separation factor (R_L) is in relation to the Langmuir isotherm and it is used to assess adsorption feasibility on the given adsorbent. It is calculated using the next Eq (15):

$$R_L = \frac{1}{(1+bC_0)}$$

(15)

where C_0 (mol dm^{-3}) is the initial adsorbate concentration, b (dm^3 mol^{-1}) is the Langmuir constant. The value of R_L points out to the isotherm type: irreversible ($R_L = 0$), favorable ($0 < R_L < 1$), linear ($R_L = 1$), unfavorable ($R_L > 1$).

Statistical analysis of the experimental data

All adsorption experiments were repeated three times and the mean values were taken for further processing and modeling. The obtained results were analyzed using the normalized standard deviation Δq (%) which is calculated using the following equation:

$$\Delta q (\%) = \sqrt{\sum \frac{[(q_{exp} - q_{cal})/q_{exp}]^2}{N-1} x100}$$

(16)

where q_{exp} and q_{cal} are the experimental and calculated values of adsorbed malathion, and N is the number of data used in the analysis. The maximum deviation is <3%, which is an experimental error. Standard errors for isothermal, kinetic, and thermodynamic parameters were determined using the commercial software Microcal Origin 8.0 (Pantić et al, 2019).

In order to confirm the adsorption model that best corresponds to the experimental data, they were analyzed by the ANOVA variance analysis, using the F value together with the values of the correlation coefficient (R) from the regression analysis. (Pantić et al, 2019; Bajić et al, 2019)

Optimization of the experimental adsorption conditions

The optimization of the adsorption conditions was performed using the RSM (Surface Response Methodology) method. Classical adsorption optimization usually involves examining the impact of each variable separately. However, it is difficult to predict optimal reaction conditions based on such results due to possible interactions between different independent variables involved in adsorption reactions. (Pantić et al, 2019; Bajić et al, 2019) Recently, various statistical programs have been used that are useful to help establish the design of the experiment. Using response surface methodology (RSM) as a mathematical function, it is possible to examine the individual and interactive influences of different variables in relation to different predictors. In that way, we get the optimal conditions that are needed to get the best results. (Pantić et al, 2019) In addition, it has been proven that the central composition design (CCD) and the Bok-Behnken design (BBD) are efficient designs of RSM models in optimizing the adsorption process. (Pantić et al, 2019) In this study, the synthesized modified adsorbent RMHAp was used to remove malathion from water. The adsorption process is optimized by numerical and graphical optimization methods using the Bok-Behnken design. We used the design with four factors (input variables) and three levels of values in which 29 experiments with five replications in the central point were performed. The capacity of the adsorbent was

PDF generated from XML JATS4R by Redalyc
Project academic non-profit, developed under the open access initiative
879

taken as a response. Extremely optimized conditions were confirmed by additional experimental testing. The conditions of the adsorption experiment are given in Table 4.

TABLE 4
An experimental malathion adsorption plan was performed
using a four-factor BBD design with three levels of value

Ordinal number	A Dose ads. (mg/L)	B t (min)	C pH	D T(^{0}C)	Response q_e (mg g^{-1})
1.	1000	95	7	45	14.1
2.	1000	95	7	25	12.6
3.	100	95	4	35	30.11
4.	550	95	4	45	12.05
5.	1000	180	7	35	15.06
6.	100	95	10	35	27.4
7.	1000	95	10	35	6
8.	550	95	10	25	9.38
9.	550	95	7	35	24.3
10.	550	10	7	25	13.2
11.	100	95	7	45	71.2
12.	100	180	7	35	81.15
13.	550	95	4	25	10.1
14.	550	10	4	35	8
15.	550	95	10	45	13.1
16.	100	10	7	35	27.3
17.	550	180	7	25	28.5
18.	550	10	7	45	14
19.	550	95	7	35	24.3
20.	1000	10	7	35	5.21
21.	550	180	7	45	28.75
22.	550	95	7	35	24.3
23.	550	180	10	35	13.8
24.	550	95	7	35	24.3
25.	550	95	7	35	24.4
26.	1000	95	4	35	6.75
27.	550	180	4	35	15.11
28.	100	95	7	25	64.4
29.	550	10	10	35	5.6

Results and discussion

Physical and chemical characterizations of adsorbents

The elemental composition of shellfish shards is given in Table 5. This elemental composition is similar to that of other authors (Wei et al, 2018; Buasri et al, 2013) and indicates that shellfish shards are mostly composed of calcium carbonate-based minerals (calcite and argonite) and the organic part of chitin that connects calcite structures. The composition of shells also includes various microelements - ions, which replace Ca^{2+} in the structure of calcium carbonate and are incorporated into the shell during its formation. The availability and rate of bioaccumulation of these ions is a function of environmental and biological factors. Thus, different habitats, contamination - the presence in the water of different ionic species, different stages of shell development can represent different patterns of metal incorporation.

TABLE 5
Concentrations of major minor and trace elements obtained
in this study using the ICPAES and ICPMS methods

Element ICP-AES Method	Ca (wt %)	Fe (wt %)	Mg (wt %)	Si (wt %)	Na (wt %)	Mn ($\mu g\ g^{-1}$)
	34.1	0.003	0.104	0.004	0.182	30.4
Element ICP-MS Method	Cd ($\mu g\ g^{-1}$)	Co ($\mu g\ g^{-1}$)	Cu ($\mu g\ g^{-1}$)	Ni ($\mu g\ g^{-1}$)	Pb ($\mu g\ g^{-1}$)	Zn ($\mu g\ g^{-1}$)
	0.094	0.079	31.2	2.01	3.09	21.5

The analyzed shards of the river shell *Anodonta Sinadonta woodiane* are composed of two polymorphs of calcium carbonate: calcite and aragonite, with calcite being the dominant form. Recent studies have found that the dominant $CaCO_3$ polymorph may be temperature dependent - aragonite deposition is at high temperature and calcite deposition is at low temperature (Kuklinski and Taylor, 2009; Ramajo et al, 2015; Krzeminska et al, 2016). The confirmation of the composition of the shells can also be seen on the spectrum of energy dispersive spectrometry (Figure 1) where the main building blocks are observed before (a) and after the modification of the shells (b). After modification, we notice the presence of phosphorus in the adsorbent, which confirms the transition of calcium carbonate to hydroxyapatite.
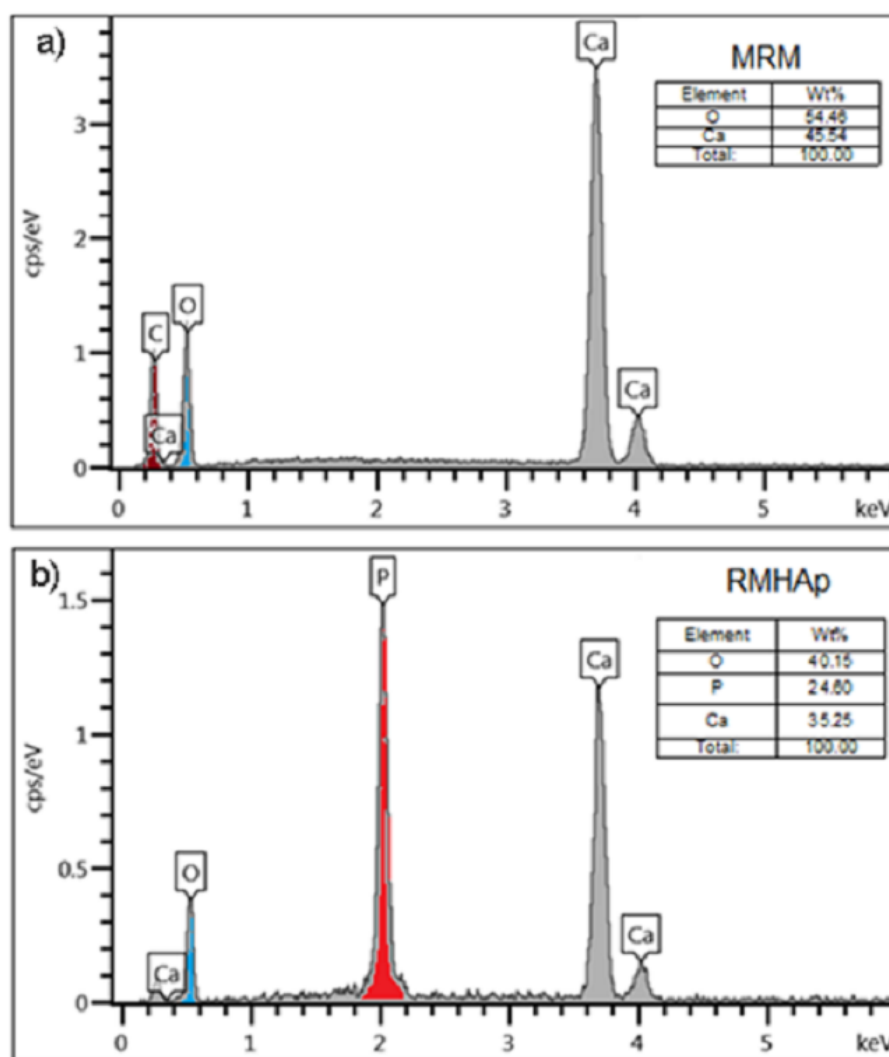
FIGURE 1
EDS spectrum of shellfish powder before (a) and after modification (b)

In the scanning electron microscopy photographs (Figure 2) with different magnifications, we can clearly see the lamellar structure of the shell. The lamellae consist of materials based on calcium carbonate (calcite and argonite) with a thickness of about 1 μm and with cavities between the lamellae with a diameter of about 50 to 100 nm. They are interconnected by organic polymer chitin; nanopores are observed on the lamellae surface.
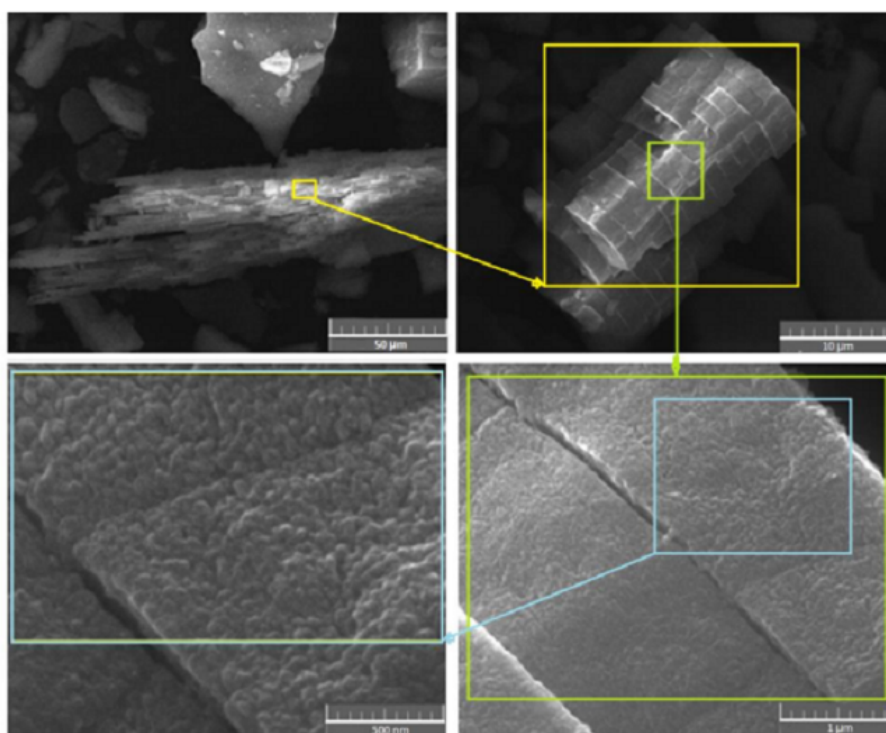
FIGURE 2
SEM representation of mechanically prepared shells at different magnifications

After mechanosynthesis, the lamellar structure derived from calcium carbonate is lost and we get the granular morphology of hydroxyapatite, presented in Figure 3. Electron scanning microscopy images showed the presence of rounded HAp microparticles in isolated and agglomerated forms. Based on the observations, HAp particles can be considered as microspheres whose crystal size is well below 1 μm.

The physical properties of the adsorbent, the specific surface area, the pore volume and the zero charge point are given in Table 6. The change in the pH_{PZC} value occurred under the influence of the change in the surface properties of the adsorbent due to modification (Table 6). At pH $<pH_{PZC}$, negatively charged species participate in electrostatic attraction with a positively charged adsorbent surface and vice versa, at pH> pH_{PZC}, electrostatic repulsion is a major factor leading to low adsorption efficiency.

FIGURE 3
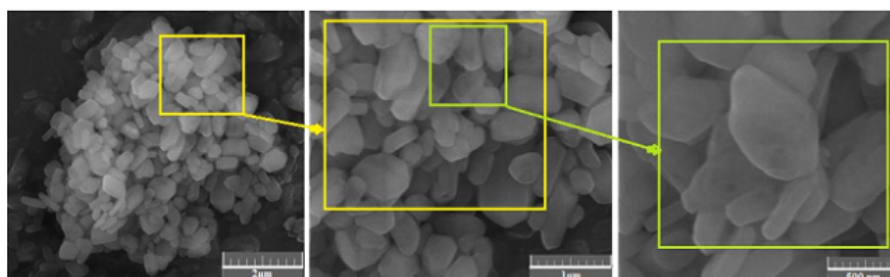SEM representation of the shells modified by mechanosynthesis at different magnifications

PDF generated from XML JATS4R by Redalyc
Project academic non-profit, developed under the open access initiative
883

TABLE 6
Physical properties of MRM and RMHAp adsorbents

Adsorbent	Specific surface area ($m^2 g^{-1}$)	Pore volume ($cm^3 g^{-1}$)	Mean pore diameter (nm)	pH_{PZC}
MRM	2,58	0,096	6,7	7,2
RMHAp	1,95	0,088	9,18	7,05

Figure 4 shows the FTIR spectra of both adsorbents (MRM and RMHAp) before and after the adsorption of malathion from aqueous solution. In the spectrum a, the characteristic peaks at 710, 856 and 1460 cm^{-1} indicate the carbonate group in the sample which confirm that the sample contains $CaCO_3$. In addition, small infrared absorption spectra are shown at $\sim$ 1790, and $\sim$ 2874 cm^{-1} and have been attributed to regimens of combining different ranges of CO_3^{2-} (Khiri et al, 2016). The spectrum at $\sim$ 1083 cm^{-1} is related to the C – O tensile vibrations as CO_2 adsorbed on the CaO surface (Khiri et al, 2016).

The FTIR spectrum (c) of the RMHAp adsorbent showed pronounced peaks at 560 cm^{-1} corresponding to the symmetrical bending regime of PO_4^{3-} and 1064 cm^{-1} corresponding to the asymmetric stretching regime of the PO_4^{3-} group corresponding to the vibrational structures of hydroxyapatite (Khiri et al, 2016). The large peak in Figure 4 in the spectrum a and a smaller peak in the spectrum c at 1460 cm^{-1} represent carbonate (CO_3), which is more pronounced before mechanosynthesis, i.e. before the conversion of calcium carbonate into hydroxyapatite.
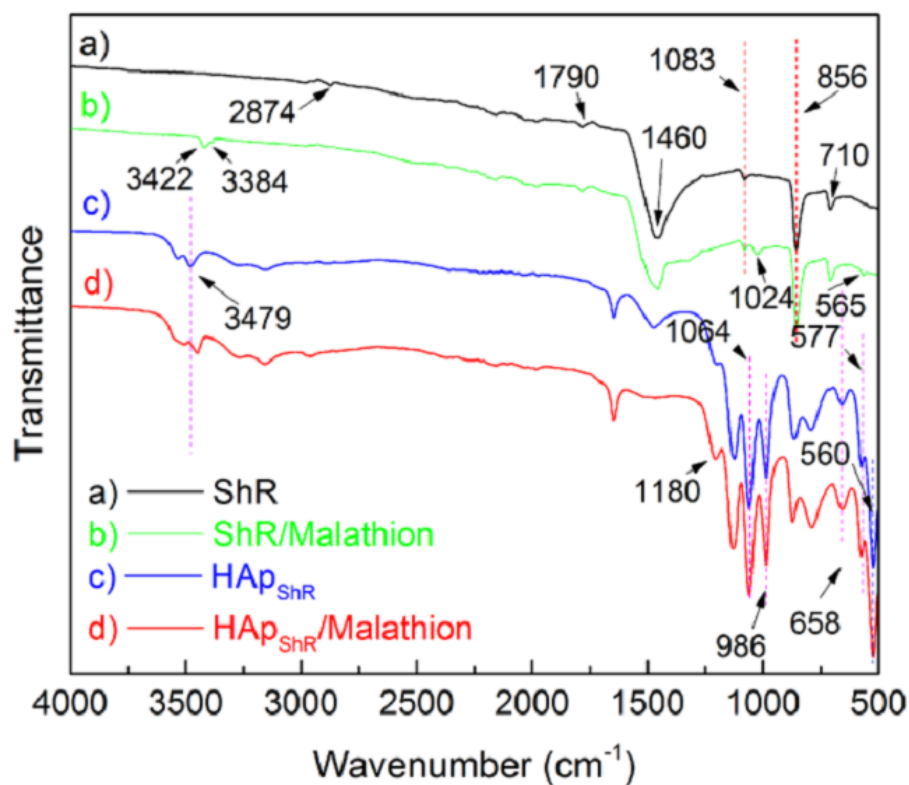
FIGURE 4
FTIR spectrum of shellfish shards and modified shards before
and after the adsorption of malathion from aqueous solution

The characteristic vibration peaks of shell dust before and after modification with a comparative review by other researchers are given in Table 7.

TABLE 7
FTIR shell powder vibration mode before and after
mechanosynthesis MRM and RMHAp and references

	Vibration frequency (cm^{-1})			
	Our research FTIR	(Khiri et al, 2016)	(Salma et al, 2010)	(Islam et al, 2013)
Symmetrical deformation CO_3^{2-}	710	708		706
Asymmetric deformations CO_3^{2-}	856, 1460	855, 1454		857, 1455
Symmetric stretching vibration CO_3^{2-}	1083	1082		1082
CO_3^{2-} deformations	1790	1786		1794
PO_4^{3-} bending	560	565	560, 599	
PO_4^{3-} stretching	1064	1024	1046	
CO_3^{2-} group	1460	1454	1424	

After sorption of malathion (spectra b and d) on both adsorbents, changes were observed in the appearance of new peaks, decrease in their intensity as well as in their disappearance and displacement.

The diffraction analysis (XRD) results showed that the composition of the river shell (spectrum a) mainly consists of two forms of $CaCO_3$, primarily calcite as shown by the diffraction peak at 2# about 29.52, 39.56, 43.27, 47.6, and 48.63 (Wei et al, 2018) and argonite (Islam et al, 2013). Other minerals are present in smaller quantities as a consequence of the uptake of these minerals from the water during shell formation. The XRD spectrum of synthesized HAp also shows relatively high intensities and sharp peaks in the range of 23–39 (about 25.80 and 32.90 (Skwarek et al, 2014) corresponding to (hkl) indices) at (002) and (300), and lower peak intensities in the range of 40–39. 60, which is consistent with the formation of the lower crystal structure of HAp.
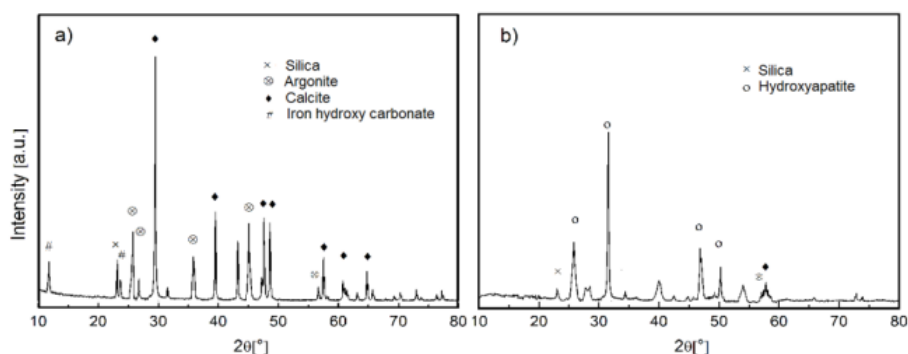

FIGURE 5
X-ray diffraction analysis (XRD) spectrum of shellfish shards
before (a) and after modification by mechanosynthesis (b)

Influence of the solution pH on adsorption

The influence of the pH value on the system is manifested through surface tension, surface properties, degree of ionization of groups present on the surface of the adsorbent, as well as through the speciation of ions in aqueous solution at a certain pH value.

The pH effect on malathion removal is presented in Figure 6. As mentioned above, malathion retention depends on the nature of the adsorbent. Removal by RMHAp adsorbent is greater than removal by MRM. Similarly to the Saib study (Bouchenafa-Saib et al, 2014), the pH value of 6 appears to be optimal for malathion sorption for both adsorbents. At this pH, H_3O^+ ions attract surface oxygenated adsorbent groups, which could lead to the formation of a bond between H_3O^+ and any doublet without malathion-sulfur. Below and above this pH value, adsorption is lower due to the hydrolysis of malathion at values higher than 8 and lower than 5 and the formation of ionic species with lower affinity for the adsorbent surface, i.e. precipitation contributes to ion removal.
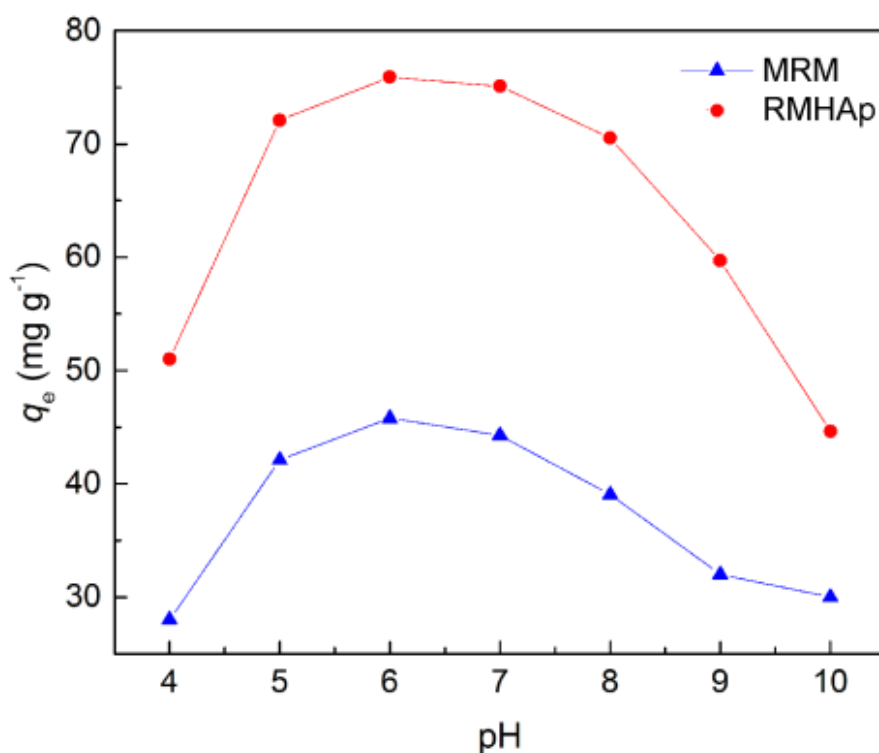

FIGURE 6
Influence of the pH value of the initial solution on malathion removal

Adsorption largely depends on the solution pH so the process itself is more favorable at medium pH values. Also in the natural environment (water) at pH values lower than 5 and higher than 8, malathion easily hydrolyzes to metabolites that are more toxic than malathion itself (Bouchard et al, 2003), which is another reason why sorption experiments are performed at pH 6.

Adsorption kinetics

The effect of time on malathion adsorption was monitored in the range of 10 to 180 minutes. The final equilibrium was established after 300 minutes but, since the difference in the removal of As (V) ions from 180 to 300 minutes ranged from 3 to 7% in order to speed up the process, we took 180 minutes as the final time.

In order to determine the kinetic model that accompanies adsorption in order to interpret the adsorption mechanism, we used pseudo-first, pseudo-second-order and second-order models (Table 3).

Table 8 shows the kinetic parameters for malathion absorption on MRM and RMHAp adsorbents.

TABLE 8

The kinetic parameters for malathion adsorption on MRM and RMHAp adsorbents ($Ci_{malathion}$ =20.32 mg L^{-1}, pH=6; m/V=100 mg L^{-1}, T= 25 ^{o}C)

Adsorbent	Model parameters	Pseudo–first	Pseudo–second	Second–order
MRM	q_e	37.247	53.589	53.589
	k (k_1, k_2)	0.01589	0.00054	0.000093
	R^2	0.960	**0.992**	0.931
RMHAp	q_e	67.425	92.142	92.142
	k (k_1, k_2)	0.02041	0.00031	0.00025
	R^2	0.074	**0.004**	0.041

The results shown in Table 8, according to the regression coefficient (R^2) and the standard error for all model parameters, indicate that the kinetics for all adsorbents is best described using a pseudo-second order model.

The rate constants of diffusion kinetic models, intra-particle diffusion, Weber-Morris, Dunwald-Wagner and homogeneous solid diffusion models for malathion adsorption on MRM and RMHAp adsorbents under the same experimental conditions are presented in Table 9.

The complex nature of the kinetics of adsorption processes can be described by observing the adsorption of all ions adsorbed on the adsorbent as a single step, as described by a pseudo-second order equation, but can also be described by consecutive / competitive steps.

The Weber-Morris model reveals two linear steps that describe the adsorption process: fast kinetics in the first step and slower in the second. The first linear part describes the external mass transfer to the adsorbent surface, while the second part describes the process of material transfer into the porous structure of the adsorbent, and strictly depends on the size and shape of the pores as well as on the density of their network on MRM and RMHAp adsorbents. Intra-particle and film diffusions slow down the transport of adsorbates. In the final phase of the process, adsorption takes place slowly until saturation is achieved on the entire available surface of the adsorbent.

PDF generated from XML JATS4R by Redalyc
Project academic non-profit, developed under the open access initiative
888

TABLE 9

Parameters of diffusion kinetic models ($Ci_{malathion}$=20.32 mg L^{-1}, pH= 6; m/V=100 mg L^{-1}, T=25 °C

Adsorbent	Model	Model parameters	Values
MRM	Weber–Morris Step 1	k_{p1} (mg g^{-1} min$^{-0.5}$)	3.6188
	(Intra–particle diffusion)	C (mg g^{-1})	3.176
		R^2	0.995
	Weber–Morris Step 2	k_{p2} (mg g^{-1} min$^{-0.5}$)	0.304
	(equilibrium)	C (mg g^{-1})	40.247
		R^2	0.999
	Dunwald–Wagner model	K	0.00711
		R^2	0.953
	Homogenous Solid Diffusion Model (HSDM)	Ds	$9.34 \bullet 10^{-12}$
		R^2	0.950
RMHAp	Weber–Morris Step 1	k_{p1} (mg g^{-1} min$^{-0.5}$)	6.792
	(Intra–particle diffusion)	C (mg g^{-1})	2.286
		R^2	0.998
	Weber–Morris Step 2	k_{p2} (mg g^{-1} min$^{-0.5}$)	0.608
	(equilibrium)	C (mg g^{-1})	67.719
		R^2	0.999
	Dunwald–Wagner model	K	0.00698
		R^2	0.956
	Homogenous Solid Diffusion Model (HSDM)	Ds	$9.24 \bullet 10^{-14}$
		R^2	0.950

Adsorption activation energy

In relation to the results of the kinetic research performed at temperatures of 298, 308, and 318 K, it is possible to determine the activation energy using the Arrhenius equation (Table 10). The linear form of the Arrhenius equation (19) is:

$$\ln K' = -\frac{E_a}{RT} + \ln A$$

(19)

where K' is the reaction rate constant at a certain temperature, E_a shows the activation energy, R is the universal gas constant (8.314), T is the temperature in K and A is the Arenius factor (frequency for a given reaction).

TABLE 10
Pseudosecond kinetic model parameters for malathion adsorption on MRM
and RMHAp adsorbents ($Ci_{malathion}$=20.32 mg L^{-1}, pH= 6; m/V=100 mg L^{-1}

Adsorbent	Temperature	q_e (mg g^{-1})	k_2 (g (mg min)$^{-1}$)	R^2
MRM	25 ^{0}C	53.594	0.000537	0.992
	35 ^{0}C	57.658	0.000636	0.992
	45 ^{0}C	62.271	0.000706	0.993
RMHAp	25 ^{0}C	92.142	0.000308	0.994
	35 ^{0}C	92.333	0.000351	0.995
	45 ^{0}C	94.224	0.000374	0.995

Physosorption or physical adsorption generally possesses energy up to 40 kJ mol^{-1}, while hemisorption requires higher energy and activation energy over 40 kJ mol^{-1} (Karanac et al, 2018). Based on the obtained results where Ea for MRM is 10.816 kJ mol^{-1} and for RMHAp 7.711 kJ mol^{-1}, we can conclude that the main mechanism of adsorption is physical adsorption.

Adsorption isotherms

The state of interactions / bonds on the surface of the adsorbate / adsorbent can be observed by fitting the experimental data with different adsorption isotherms. The normalized correlation coefficient and standard deviation were used to estimate the fit of the adsorption data.

The experimental data were compared with the Langmuir, Freundlich, Temkin, and Dubinin-Radushkevich isotherm models already discussed, the parameters of which are shown in Table 11. By analyzing the experimental data on the adsorption of malathion molecules on the tested adsorbents, the best fit for both adsorbents is given by the Freundlich isothermal model. The results of modeling malathion adsorption on the tested adsorbents are given in Table 11.

TABLE 11

Parameters of the adsorption isotherms of malathion adsorption on MRM and RMHAp adsorbents

Adsor-bent	Isothermal models and parameters		Temperature		
			25 °C	35 °C	45 °C
MRM	Langmuir isotherm	q_m (mg g^{-1})	46.462	48.135	49.789
		K_L (L mg^{-1})	1.918	1.968	2.027
		K_L (L mol^{-1})	633570	650164	669551
		R^2	0.992	0.994	0.995
	Freundlich isotherm	K_F (mg g^{-1}) (dm^3 mg^{-1})$^{1/n}$	28.469	29.252	30.066
		$1/n$	0.182	0.189	0.195
		R^2	**0.997**	**0.998**	**0.988**
	Temkin isotherm	A_T (dm^3 g^{-1})	443.06	376.95	329.44
		b_T	4.95	5.25	5.54
		R^2	0.980	0.980	0.978
	Dubinin-Radushkovich isotherm	q_m (mg g^{-1})	34.25	35.18	36.12
		K_{ad} (mol^2 kJ^{-2})	9.17	9.15	9.12
		Ea (kJ mol^{-1})	7.38	7.39	7.40
		R^2	0.802	0.796	0.791
RMHAp	Langmuir isotherm	q_m (mg g^{-1})	78.311	84.502	87.485
		K_L (L mg^{-1})	1.531	1.614	1.715
		K_L (L mol^{-1})	505829	533409	566567
		R^2	0.980	0.982	0.985
	Freundlich isotherm	K_F (mg g^{-1}) (dm^3 mg^{-1})$^{1/n}$	39.432	42.473	44.313
		$1/n$	0.275	0.279	0.289
		R^2	**0.998**	**0.996**	**0.987**
	Temkin isotherm	A_T (dm^3 g^{-1})	80.959	100.297	99.368
		b_T	10.03	10.17	11.05
		R^2	0.938	0.933	0.958
	Dubinin-Radushkovich isotherm	q_m (mg g^{-1})	47.82	49.48	51.05
		K_{ad} (mol^2 kJ^{-2})	8.84	8.81	8.78
		Ea (kJ mol^{-1})	7.52	7.53	7.55
		R^2	0.792	0.766	0.766

According to the Freundlich isotherm, the mechanism of ion adsorption on MRM and RMHAp can be described as heterogeneous adsorption, where the adsorbed ions / molecules have different enthalpies and adsorption activation energies. The value of n from the Freundlich isotherm is a measure of adsorption intensity or surface heterogeneity. Values of n near zero indicate a highly heterogeneous surface. Values of n <1 (Table 11) imply a hemisorption process, and higher values indicate combined adsorption, e.g. physisorption and hemisorption with different process contributions at different system balancing steps. The values in Table 11 indicate that the adsorption was combined in all cases.

The calculation of the separation factor (R.) according to equation (20) which is based on the parameter b of the Langmir isotherm indicates the feasibility of adsorption on a given adsorbent. It is calculated using the following equation:

$$R_L = \frac{1}{(1 + bC_0)}$$

(20)

where C_0 (mol L^{-1}) is the initial adsorbate concentration and b (L mol^{-1}) is the Langmir constant. The value of R_L indicates the feasibility of the adsorption process: irreversible ($R_L = 0$), favorable ($0 < R_L < 1$), linear ($R_L = 1$), and unfavorable ($R_L > 1$). The R_L for adsorption of malathion ions on MRM ranges from 0.023 to 0.204 and for RMHAp from 0.027 to 0.243 indicating that the adsorption process is favorable.
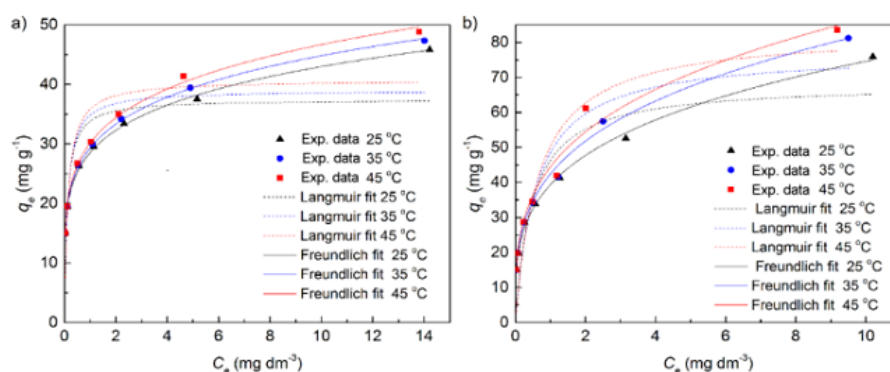

FIGURE 7
Review of the results of the adsorption experiments with the best-fitting models of isotherms
(solid line) for the removal of malathion on adsorbents MRM (a) and RMHAp (b)

Thermodynamic studies

Gibbs free energy (ΔG^0), enthalpy (ΔH^0) and entropy (ΔS^0) were calculated by Van't Hoff equation (21) and (22):

$$\Delta G^0 = -RT \, ln(b)$$

(21)

$$ln(b) = \frac{\Delta S^0}{R} - \frac{\Delta H^0}{(RT)}$$

(22)

where T is the absolute temperature in K, R is the universal gas constant (8.314 mol^{-1} K^{-1}) and the adsorption constant b is calculated using the Langmir isotherm (Table 12). ΔH^0 and ΔS^0 were calculated from the slope and the sections in the diagram $ln(b)$ - T^{-1}, assuming that the adsorption kinetics values are stationary. The calculated thermodynamic parameters are shown in Table 12.

TABLE 12
Calculated Gibbs free adsorption energy, enthalpy and entropy for
malathion adsorption on MRM, and RMHAp at 25, 35, and 45 °C

Adsorbent	$\Delta G°$ (kJ mol^{-1})			$\Delta H°$ (kJ mol^{-1})	$\Delta S°$ (J mol^{-1} K^{-1})	R^2
	25 ^{0}C	35 ^{0}C	45 ^{0}C			
MRM	-43.07	-44.58	-46.11	2.18	151.75	0.996

Negative values of Gibbs free energy ($\Delta G°$) and positive values of entropy ($\Delta S°$) at all temperatures indicate that reactions in the adsorption process take place spontaneously. A decrease in the Gibbs free energy ($\Delta G°$) with an increase in temperature also indicates that the spontaneity of the reaction increases.

Positive values of ΔS^0 indicate a tendency of greater disorder of the MRM and RMHAp surface systems and malathion solution. In Table 12, we can see that the Gibbs free energy values ($\Delta G°$) for both adsorbents are approximate, and the positive entropy values ($\Delta S°$) at all temperatures, while the positive enthalpy values (ΔH^0) for MRM and RMHAp are noticeable, which indicates the endothermic process. In general, the exchange of free energy in the case of physisorption is somewhere between -20 and 0 kJ mol^{-1}, for simultaneous hemisorption and physisorption between -20 and -80 kJ mol^{-1}, and hemisorption less than -80 kJ mol^{-1}. The obtained results indicate that in these cases, hemisorption and physisorption are present at the same time.

Optimization of adsorption conditions

The individual interaction and the impact of various variables in relation to different predictors were tested using the response surface methodology (RSM) as a mathematical function by commercial software design Expert 9. The mutual influence of the input variables was analyzed by analyzing the variances of ANOVA using the quadratic model of the equation shown in Table 13.

TABLE 13

ANOVA variance analysis for a square response surface model for the removal of malathion from water using the RMHAp adsorbent

Source	Sum of square	df	Mean Square	F Value	p-value Prob > F
Model	9102.20579	14	650.1575566	8.986135	0.0001 significant
A-dose adsorbent	4873.88213	1	4873.882133	67.36423	< 0.0001
B-t	991.173633	1	991.1736333	13.69948	0.0004
C-pH	3.8988	1	3.8988	0.053887	0.8198
D-T	18.8000333	1	18.80003333	0.259844	0.6182
AB	484	1	484	6.689593	0.0215
AC	0.9604	1	0.9604	0.013274	0.9099
AD	7.0225	1	7.0225	0.097061	0.7600
BC	0.297025	1	0.297025	0.004105	0.9498
BD	0.075625	1	0.075625	0.001045	0.9747
CD	0.783225	1	0.783225	0.010825	0.9186
A^2	756.17519	1	756.1751903	10.45145	0.0060
B^2	37.4530282	1	37.45302815	0.517656	0.4837
C^2	1399.36149	1	1399.361488	19.34124	0.0006
D^2	27.51492	1	27.51492005	0.380297	0.5473
Residual	1012.91668	14	72.35119167		
Lack of Fit	1012.90868	10	101.2908683	50645.43	< 0.0001 significant
Pure Error	0.008	4	0.002		
Cor Total	10115.1225	28			

A graph of the optimal conditions with respect to the input variables for removing malathion from water using RMHAp is shown in Figure 7.
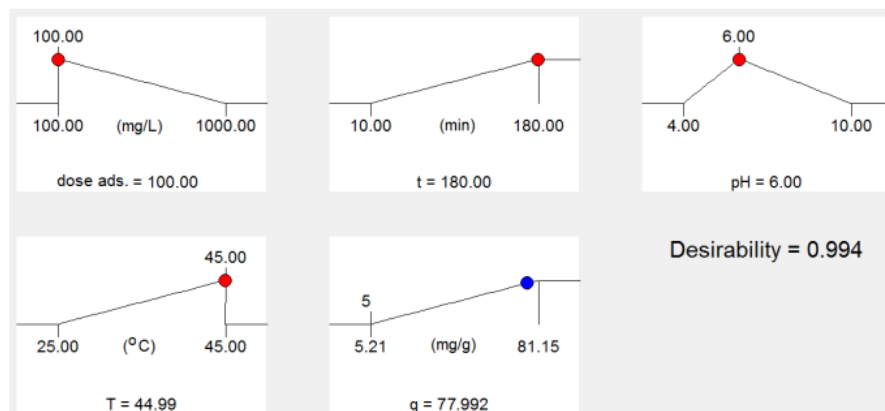

FIGURE 8

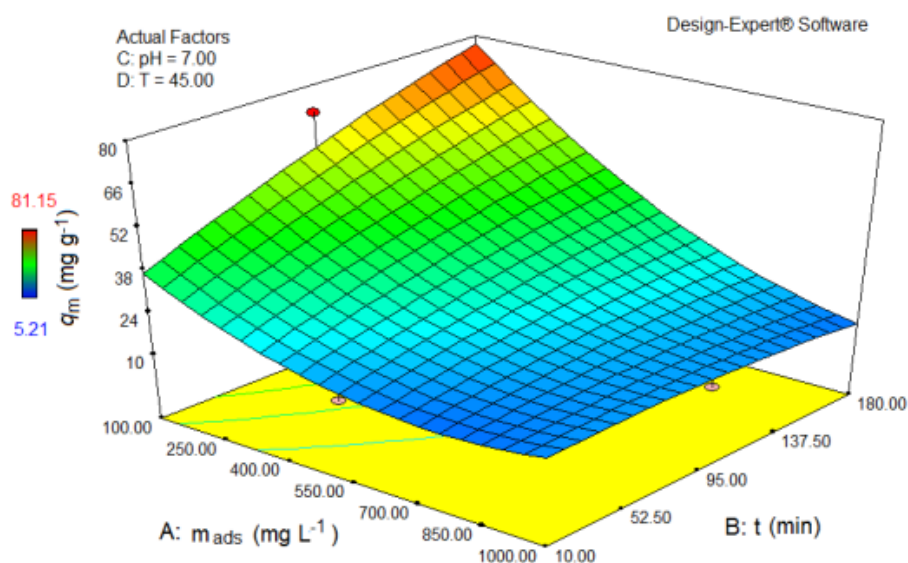Optimization of the input parameters in relation to the maximum capacity of the adsorbent

FIGURE 9
3D diagram of the mutual interactions of dependence
of significant input variables (adsorbent dose and time)

Conclusion

MRM and RMHAP showed excellent malathion removal performance. The results of isothermal, kinetic, and thermodynamic studies suggested simultaneous physisorption and hemisorption between malathion molecules and the surface of MRM and RMHAP adsorbents during the adsorption process. The optimal parameters for the maximum malathion adsorption were: system pH value - 6, adsorbent dose - 100 mg L^{-1}, adsorption time - 180 minutes, and temperature - 45 °C. Adsorption was spontaneous and endothermic as described by thermodynamic parameters. The Bok-Behnken's design within the response surface method has been successfully used in the optimization of experimental adsorption conditions, the goal of optimization being to determine the optimal adsorption conditions with a smaller number of experiments. Optimization methods are maximally harmonized with the principles of environmental protection thus reducing: the number of experiments, the amount of consumed expensive and environmentally harmful chemicals, and the generation of waste. The errors and the predicted response values, derived from a mathematical model, showed acceptable results and confirmed the favorable effect of the studied factors on malathion adsorption using RMHAP. This paper investigates the sustainable use of biowaste for the treatment of water contaminated with organophosphorus pesticides, whereby the biowaste that burdens the banks of rivers is used to remove water pollutants, thus leading to a double benefit for the environment.

References

Bajić, Z.J., Djokić, V.R., Veličković, Z.S., Vuruna, M.M., Ristić, M.Đ., Issa, N.B. & Marinković, A.D. 2013. Equilibrium, kinetic and thermodynamic studies on removal of Cd(II), Pb(II) and As(V) from wastewater using carp (*Cyprinus Carpio*) scales. *Digest Journal of Nanomaterials and Biostructures*, 8(4), pp.1581-1590 [online]. Available at: https://chalcogen.ro/1581_Bajic.pdf [Accessed: 15 June 2021].

Bajić, Z.J., Pamučar, D.S., Bogdanov, J.Đ., Bučko, M.M. & Veličković, Z.S. 2019. Optimization of arsenite adsorption on hydroxy apatite based adsorbent using adaptive neuro-fuzzy inference system. *Vojnotehnički glasnik/Military Technical Courier,* 67(4), pp.735-752. Available at: https://doi.org/10.5937/vojtehg67-21519.

Bouchard, M., Gosselin, N.H., Brunet, R.C., Samuel, O., Dumoulin, M-J. & Carrier, G. 2003. A toxicokinetic model of malathion and its metabolites as a tool to assess human exposure and risk through measurements of urinary biomarkers. *Toxicological Sciences*, 73(1), pp.182-194. Available at: https://doi.org/10.1093/toxsci/kfg061.

Bouchenafa-Saïb, N., Mekarzia, A., Bouzid, B., Mohammedi, O., Khelifa, A., Benrachedi, K. & Belhaneche, N. 2014. Removal of malathion from polluted water by adsorption onto chemically activated carbons produced from coffee grounds. *Desalination and Water Treatment,* 52(25-27), pp.4920-4927. Available at: https://doi.org/10.1080/19443994.2013.808845.

Buasri, A., Chaiyut, N., Loryuenyong, V., Worawanitchaphong, P. & Trongyong S. 2013. Calcium Oxide Derived from Waste Shells of Mussel, Cockle, and Scallop as the Heterogeneous Catalyst for Biodiesel Production. *The Scientific World Journal,* 2013(art.ID:460923). Available at: https://doi.org/10.1155/2013/460923.

Budimirović, D., Veličković, Z.S., Djokić, V.R., Milosavljević, M., Markovski, J., Lević, S. & Marinković, A.D. 2017. Efficient As(V) removal by -FeOOH and -FeOOH/-MnO2 embedded PEG-6-arm functionalized multiwall carbon nanotubes. *Chemical Engineering Research and Design*, 119, pp.75-86. Available at: https://doi.org/10.1016/j.cherd.2017.01.010.

Chatterjee, S., Das, S.K., Chakravarty, R., Chakrabarti, A., Ghosh, S. & Guha, A.K. 2010. Interaction of malathion, an organophosphorus pesticide with Rhizopus oryzae biomass. *Journal of Hazardous Materials,* 174(1-3), pp.47-53. Available at: https://doi.org/10.1016/j.jhazmat.2009.09.014.

Gao, Z., Bandosz, T.J., Zhao, Z., Han, M. & Qiu J. 2009. Investigation of factors affecting adsorption of transition metals on oxidized carbon nanotubes. *Journal of Hazardous Materials,* 167(1-3), pp.357-365. Available at: https://doi.org/10.1016/j.jhazmat.2009.01.050.

Hameed, B.H., Salman, J.M. & Ahmad, A.L. 2009. Adsorption isotherm and kinetic modeling of 2,4-D pesticide on activated carbon derived from date stones. *Journal of Hazardous Materials,* 163(1), pp.121-126. Available at: https://doi.org/10.1016/j.jhazmat.2008.06.069.

Islam, K.N., Ali, M.E., Bakar, M.Z., Loqman, M.Y., Islam, A., Islam, M.S., Rahman, M.M. & Ullah, M. 2013. A novel catalytic method for the synthesis of spherical aragonite nanoparticles from cockle shells. *Powder Technology,* 246, pp.434-440. Available at: https://doi.org/10.1016/j.powtec.2013.05.046.

Kamga, F.T. 2019. Modeling adsorption mechanism of paraquat onto Ayous (*Triplochiton scleroxylon*) wood sawdust. *Applied Water Science,* 9(art.number:1). Available at: https://doi.org/10.1007/s13201-018-0879-3.

Karanac, M., Đolić, M., Veljović, Đ., Rajaković-Ognjanović, V., Veličković, Z., Pavićević, V. & Marinković A. 2018. The removal of Zn^{2+}, Pb^{2+}, and As(V) ions by lime activated fly ash and valorization of the exhausted adsorbent. *Waste Management*, 78, pp.366-378. Available at: https://doi.org/10.1016/j.wasman.2018.05.052.

Khiri, M.Z.A., Matori, K.A., Zainuddin, N., Abdullah, C.A.C., Alassan, Z.N., Baharuddin, N.F. & Zaid M.H.M. 2016. The usability of ark clam shell (Anadara granosa) as calcium precursor to produce hydroxyapatite nanoparticle via wet chemical precipitate method in various sintering temperature. *SpringerPlus*, 5(art.number: 1206). Available at: https://doi.org/10.1186/s40064-016-2824-y.

Krzeminska, M., Kuklinski, P., Najorka, J. & Iglikowska, A. 2016. Skeletal Mineralogy Patterns of Antarctic Bryozoa. *Journal of Geology*, 124(3). Available at: https://doi.org/10.1086/685507.

Kuklinski, P. & Taylor P.D. 2009. Mineralogy of Arctic bryozoan skeletons in a global context. *Facies,* 55, pp.489-500. Available at: https://doi.org/10.1007/s10347-009-0179-3.

Ohno, K., Minami, T., Matsui, Y. & Magara, Y. 2008. Effects of chlorine on organophosphorus pesticides adsorbed on activated carbon: desorption and oxon formation. *Water Research,* 42(6-7), pp.1753-1759. Available at: https://doi.org/10.1016/j.watres.2007.10.040.

Pantić, K., Bajić, Z.J., Veličković, Z.S., Djokić, V., Rusmirović, J., Marinković, A. & Perić-Grujić, A. 2019. Adsorption performances of branched aminated waste polyacrylonitrile fibers: experimental versus modelling study. *Desalination and Water Treatment*, 171, pp.223-249. Available at: https://doi.org/10.5004/dwt.2019.24758.

Perendija, J., Veličković, Z.S., Cvijetić, I., Lević, S., Marinković, A., Milošević, M. & Onjia, A. 2021. Bio-membrane based on modified cellulose, lignin, and tannic acid for cation and oxyanion removal: Experimental and theoretical study. *Process Safety and Environmental Protection*, 147, pp.609-625. Available at: https://doi.org/10.1016/j.psep.2020.12.027.

Ramajo, L., Rodriguez-Navarro, A.B., Duarte, C.M., Lardies, M.A. & Lagos, N.A. 2015. Shifts in shell mineralogy and metabolism of Concholepas concholepas juveniles along the Chilean coast. *Marine and Freshwater Research*, 66(12), pp.1147-1157. Available at: https://doi.org/10.1071/MF14232.

Salma, K., Berzina-Cimdina, L. & Borodajenko, N. 2010. Calcium phosphate bioceramics prepared from wet chemically precipitated powders. *Processing and Application of Ceramics,* 4(1), pp.45-51. Available at: https://doi.org/10.2298/PAC1001045S.

Singh, V.K., Singh, R.S., Tiwari, P.N., Singh, J.K., Gode, F. & Sharma, Y.C. 2010. Removal of Malathion from Aqueous Solutions and Waste Water Using Fly Ash. *Journal of Water Resource and Protection*, 2(4), pp.322-330. Available at: https://doi.org/10.4236/jwarp.2010.24037.

Skwarek, E., Janusz, W. & Sternik, D. 2014. Adsorption of citrate ions on hydroxyapatite synthetized by various methods. *Journal of Radioanalytical and Nuclear Chemistry*, 299, pp.2027-2036 Available at: https://doi.org/10.1007/s10967-013-2825-z.

Stevanović, M., Bajić, Z.J., Veličković, Z.S., Karkalić, R., Pecić, Lj., Otrisal, P.& Marinković, A. 2020. Adsorption performances and antimicrobial activity of the nanosilver modified montmorillonite clay. *Desalination and Water Treatment*, 187, pp.345-369. Available at: http://dx.doi.org/10.5004/dwt.2020.25451

Taleb, K., Markovski, J., Milosavljević, M., Marinović-Cincović, M., Rusmirović, J., Ristić, M. & Marinković, A., 2015. Efficient arsenic removal by cross-linked macroporous polymer impregnated with hydrous iron oxide: material performance. *Chemical Engineering Journal,* 279, pp.66-78. Available at: https://doi.org/10.1016/j.cej.2015.04.147.

Taleb, K., Markovski, J., Veličković, Z., Rusmirović, J., Rančić, M., Pavlović, V. & Marinković, A. 2019. Arsenic removal by magnetite-loaded aminomodified nano/microcellulose adsorbents: Effect of functionalization and media size. *Arabian Journal of Chemistry*, 12(8), pp.4675-4693. Available at: https://doi.org/10.1016/j.arabjc.2016.08.006.

Wei, D., Zhang, H., Cai, L., Guo, J., Wang, Y., Ji, L. & Song, W. 2018. Calcined Mussel Shell Powder (CMSP) via Modification with Surfactants: Application for Antistatic Oil-Removal. *Materials*, 11(8), 1410. Available at: https://doi.org/10.3390/ma11081410.

Funding

Additional information

FIELD: Environmental protection, Chemical engineering

ARTICLE TYPE: Original scientific paper

Alternative link

https://scindeks.ceon.rs/article.aspx?artid=0042-84692104871V (html)
https://scindeks-clanci.ceon.rs/data/pdf/0042-8469/2021/0042-84692104871V.pdf (pdf)